Acta Geophysica (2020) 68:1753–1762
https://doi.org/10.1007/s11600-020-00505-1

RESEARCH ARTICLE - APPLIED GEOPHYSICS

Periods of refracted P-waves in coal seams and their applications in coal thickness estimations

Zuiliang Liu[1,2] · **Ji Wang**[3]

Received: 3 June 2020 / Accepted: 28 October 2020 / Published online: 17 November 2020

Abstract

The direct and accurate estimations of coal thicknesses are prerequisites for intelligent mining practices. One of the most effective methods for detecting the distributions of coal thicknesses in coal mining panels is the in-seam seismic (ISS) method. In the present study, after examining the formation processes and propagation characteristics of refracted P-waves in ISS data, it was concluded that the refracted P-waves in coal seams are mainly formed by the multiple transmission and reflection of the P-waves between the coal and rock interfaces of roof and floor at critical angles. This results in the refracted P-waves having strong periodicity, and these periods are proportional to the coal thicknesses. This study adopted numerical simulation models with different coal thicknesses, and the aforementioned periodicity characteristics were examined. It was found that the coal seam thicknesses could be calculated using the periods of the refracted P-waves. However, in thin- or medium-thick coal seams, it was found that multiple transmitted P-waves overlapped and the periods could not be read directly. Therefore, in order to solve this problem, this study composed source wavelets with the main frequency of the source signals and then composite synthetic P-waves by convoluting the source wavelets with the sequences of various coal thicknesses. The suitable estimated coal thickness corresponded to the minimum value of the errors between the synthetic and actual refracted P-waves. An experiment was conducted in the No. 42224 panel of the Chaigou Coal Mine in order to validate the proposed method. The experimental results revealed that the estimated coal thicknesses from the refracted P-waves were consistent with the actual geologic conditions in the coal mine. Due to the fact that the refracted P-waves arrive earlier than other waves in seismic records, the refracted P-waves could be easily identified and processed. Overall, the proposed method was found to be a simple application process for accurate coal thickness estimations.

Keywords Refracted P-wave · Coal seam thickness · In-seam seismic

Introduction

The methods currently applied in coal mining processes are moving toward intelligent choices which require the shearing or tunneling systems to predict the altitudes of the interfaces between coal seams and rock strata in order to adjust cutting heights in advance (Wang et al. 2020a). During these processes, the accurate detections of the coal seam thicknesses are one of the preconditions of the interface predictions (Wang et al. 2011). At the present time, there are two geophysical methods which have the ability to underground detect the thicknesses of coal seams, geological radar (Liu et al. 2019) and in-seam seismic (ISS) methods (Zhu et al. 2019). The principle of ISS thickness detection is based on the differences in dispersions and amplitude attenuations when the in-seam waves propagate in coal seams with different thicknesses. Therefore, ISS methods can be subdivided into the tomographic methods based on amplitude attenuations (Ji et al. 2014) and the inversion methods based on dispersion curves (Hu et al. 2018).

The velocities of the P-waves and S-waves in coal seams are significantly lower than those of surrounding rock. When

Editorial Responsibility: Michal Malinowski (CO-EDITOR-IN-CHIEF)/Rafał Czarny (ASSOCIATE EDITOR).

✉ Ji Wang
wangji@cctegxian.com

Zuiliang Liu
liuzuiliang@163.com

[1] School of Resources and Geosciences, China University of Mining and Technology, Xuzhou, China

[2] Yangquan Coal Industry (Group) Co., Ltd., Yangquan, China

[3] Xi'an Research Institute of China Coal Technology and Engineering Group Corp., Xi'an, China

seismic waves propagate in coal seams, they will reflect and interfere repeatedly between the coal and rock interfaces of roof and floor forming in-seam waves. In previous related studies, Krey (1963) theoretically examined the origins of in-seam waves and presented a dispersion formula for them. According to the formula, under the conditions of unchanged velocities of the coal seams and surrounding rock, the frequencies and velocities of Airy phases can be determined by the coal thicknesses (RÄDer et al. 1985). Therefore, the thicknesses can be estimated by calculating frequencies and velocities of Airy phases from the ISS data and comparing them with the theoretical dispersion curves of different coal thicknesses (Hu et al. 2018). On that basis, Schott and Waclawik (2015) used the correspondence between the thicknesses and velocities to convert the velocity tomography into the distributions of coal seam thicknesses in the panels. However, this method requires high data quality. The actual underground seismic data tend to be seriously interfered with many types of noise. As a result, it has proven difficult to accurately determine the frequency and velocity values of Airy phases from actual data, producing errors to the corresponding results of the thickness estimations. Another method commonly used to estimate the coal thicknesses involves examining the amplitudes of the in-seam waves (Buchanan 1978). This method determined the tomographic attenuation coefficient of the in-seam wave amplitudes and then interprets the thicknesses according to the correlations between the attenuation coefficients and the coal seam thicknesses (Ji et al. 2014). This method has been found to be suitable for actual data with relatively low SNR. However, the thicknesses can only be roughly estimated at the present time due to the many complex factors affecting the attenuation of in-seam wave amplitudes.

Underground seismic data include not only in-seam waves, but also P-waves and S-waves (Yancey et al. 2007). In this research study, only P-waves are discussed. Differing from the P-waves in one or two layers, the P-waves in the coal seams which are surrounded by rock have long-wave trains. This is due to the fact that the P-waves propagate along the coal–rock interfaces and are guided by the coal seams. For that reason, the P-waves in the coal seams are also referred to as P–P interference waves or P-guided waves (Zhang et al. 2019). It has been observed that when P-waves propagate along the coal–rock interfaces, they will simultaneously refract to the coal seams and can be received by detectors installed in coal mines. Consequently, these waves are also referred to as refracted P-waves (Krey 1963; Regueiro 1990). Refracted P-waves are characterized by highest velocities in ISS recordings. Due to the fact that they arrive first at the detectors and do not interfere with other types of waves, they are very easy identify and process. Similar to in-seam waves, refracted P-waves can also be used to detect abnormal structures. For example, changes in velocity or amplitude can be used for the tomographic images of a panel (Gritto 2003; Wang et al. 2020b), or the reflected waves are identify to detect any structures located in front of tunnel faces (Liu et al. 2019).

In this study, the propagations of the P-waves in coal seams were discussed and the relationships between the coal seam thicknesses and the periods of refracted P-waves were investigated. This study's results were verified using numerical simulation models with different coal seam thicknesses. It was found that in thin- or medium-thick coal seams, multiple transmitted P-waves had overlapped, resulting in the periods not being able to be observed directly. Therefore, an alternative method was proposed in this study to estimate the thicknesses, and the results were verified by both simulation data and actual data.

Theoretical analysis

It has been observed that when P-waves propagate from coal seam to rock stratum, transmission and reflection of P-wave will occur at the interface. During those processes, the wave velocity in the coal v_1, wave velocity in the rock v_2, incident angle α_i, and transmission angle α_t will meet Snell's law as follows (Sheriff and Geldart 1995):

$$\frac{v_1}{\sin \alpha_i} = \frac{v_2}{\sin \alpha_t} = v, \tag{1}$$

where v is the apparent velocity of the P-wave propagating along the interface. As $v_2 > v_1$, so $\alpha_t > \alpha_i$, which means that the transmission angle is larger than the incident angle. Then, as the distance between the source and the incident point increases, the incident angle and the transmission angle will also increase. When the transmission angle increases to a right angle, the incident angle at that time is referred to as the critical angle. If the incident angle is larger than the critical angle, then the transmission angle becomes a complex, and the in-seam waves are formed by the reflection waves. In addition, if the incident angle is equal to the critical angle, the transmission angle is a right angle, and the transmission wave propagates along with the coal–rock interface with the velocity v_2. Therefore, it can be assumed that the waves will propagate at the high velocity v_2 on the rock side of the interfaces and at the low velocity v_1 on the coal side. When the high-speed waves pass through the interface, they will simultaneously produce refracted waves in the coal seam. These waves are refracted from the coal–rock interfaces to the coal seam at v_1 until they are received by receivers. However, since the distances between the source and the detectors tend to be much larger than the thicknesses of the coal seam, the propagation of the waves in the coal can be neglected. Therefore, the apparent velocity of the

refracted waves will be equal to the velocity of the waves propagating at the coal–rock interface.

When P-waves incident to a coal–rock interface, there are four types of waves generated: transmitted P-wave; reflected P-wave; transmitted SV-wave; and reflected SV-wave. The Zoeppritz equation gives the relationship between the incident angle and the amplitude changes of the different types of waves as follows (Sheriff and Geldart 1995):

$$\begin{bmatrix} -\sin\alpha_i & -\cos\beta_i & \sin\alpha_t & \cos\beta_t \\ \cos\alpha_i & -\sin\beta_i & \cos\alpha_t & -\sin\beta_t \\ \sin 2\alpha_i & \frac{v_{p1}}{v_{s1}}\cos 2\beta_i & \frac{\rho_2 v_{s2}^2 v_{p1}}{\rho_1 v_{s1}^2 v_{p2}}\sin 2\alpha_t & \frac{\rho_2 v_{s2} v_{p1}}{\rho_1 v_{s1}^2}\cos 2\beta_t \\ -\cos 2\beta_i & \frac{v_{s1}}{v_{p1}}\sin 2\beta_i & \frac{\rho_2 v_{p2}}{\rho_1 v_{p1}}\cos 2\beta_t & -\frac{\rho_2 v_{s2}}{\rho_1 v_{p1}}\sin 2\beta_t \end{bmatrix} \begin{bmatrix} R_{pp} \\ R_{ps} \\ T_{pp} \\ T_{ps} \end{bmatrix} = \begin{bmatrix} \sin\alpha_i \\ \cos\alpha_i \\ \sin 2\alpha_i \\ \cos 2\beta_i \end{bmatrix}, \tag{2}$$

where for the P-wave, the incident angle and reflection angle are all α_i, the transmission angle is α_t, the velocity in the coal is v_{p1}, and the velocity in rock is v_{p2}; for the SV-wave, the reflection angle is β_i, the transmission angle is β_t, the velocity in the coal is v_{s1}, and the velocity in rock is v_{s2}; ρ_1 and ρ_2 are the densities of coal and rock, respectively. T_{pp} is the transmission coefficient of the P-wave, which represents the ratio of the amplitude of the transmitted P-wave to that of the incident P-wave. Correspondingly, R_{pp} is the reflection coefficient of the P-wave; T_{ps} is the transmitted coefficient of the SV-wave; and R_{ps} is the reflection coefficient of the SV-wave.

Therefore, in accordance with the Zoeppritz equation, this study analyzed the relationships among the transmission coefficient T_{pp}, reflection coefficient R_{pp} and incident angle α_i of the P-waves. Model with parameters is shown in Table 1. In addition, using Eq. (1), α_t, β_i and β_t are calculated from α_i and then substituted into Eq. (2) in order to obtain T_{pp} and R_{pp}. The results are shown in Fig. 1.

As can be seen in Fig. 1, when the incident angle was smaller than the critical angle, T_{pp} and R_{pp} are about 0.5. When the incident angle was similar to the critical angle, these two coefficients increased rapidly. They were observed to reach the maximum values when the incident angle was equal to the critical angle. Next, they rapidly decreased, but R_{pp} increased again to form total reflections. It can be seen that for the P-waves, only when the incident angles were equal to the critical angle where the transmitted and reflected waves are the strongest. However, if the incident angles were insufficient or exceeded the critical angles, then the amplitudes of the transmitted and reflected waves had decayed rapidly. Therefore, the refracted P-waves were mainly generated by the P-wave incidents at the critical angles. Meanwhile, wave incidents at other angles had been attenuated. In addition, since the value of R_{pp} at the critical angle was close to 1, or even greater than 1, it could be considered that the amplitudes of the transmitted and reflected waves were not attenuated, but were enhanced under the condition of critical angles.

Only considered the incident, transmitted and reflected P-waves at the critical angle condition, the propagation

Table 1 Parameters of the model

Layer	P-wave velocity (m/s)	S-wave velocity (m/s)	Density (g/cm^3)
Roof and floor strata	3700	2100	2.7
Coal seam	2000	1100	1.3

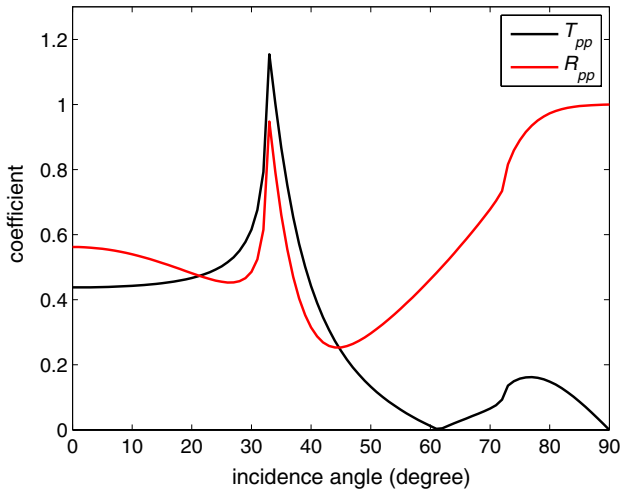

Fig. 1 Transmission coefficient T_{pp} and reflection coefficient R_{pp} for the various degrees of the incident angles

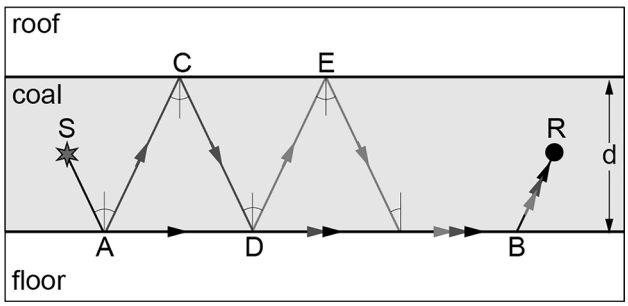

Fig. 2 Multiple transmissions and reflections of the P-wave between the coal–rock interfaces

process of a refracted P-wave in an ideal coal seam with homogeneous surrounding rock is shown in Fig. 2. As can be seen in this figure, the P-wave was excited at Point S. Then, at Point A, the wave was an incident of the coal–rock interface at the critical angle α and generated the transmitted and reflected waves. The transmitted wave propagated to Point B along the coal–rock interface at the velocity v_{p2}. During the propagation process, it was continuously refracted to the coal seam. The refracted wave at Point B propagated to the coal seam with the refraction angle α and was received by the detector located at Point R in the coal seam. The reflected wave generated at Point A also propagated at velocity v_{p1} in the coal seam with the reflection angle α. After arriving at Point C on the other coal–rock interface, this wave was again reflected with the reflection angle α and continued to propagate at v_{p1} in the coal seam. Subsequently, when it reached Point D, transmission and reflection occurred once again due to the incident angle still being the critical angle, and the transmission wave continued to propagate along the coal–rock interface at v_{p1}. Therefore, the refracted P-wave received by the detector was the result of multiple transmissions and reflections between the two coal–rock interfaces. Therefore, by assuming that the thickness of the coal seam was d, the time difference T between the two arrived P-waves can be obtained according to the geometric relationships between the rays, as detailed in Fig. 2.

$$T = 2d\frac{\sqrt{v_2^2 - v_1^2}}{v_1 v_2}. \tag{3}$$

Then, according to Eq. (3), the refracted P-wave received in the coal seam was considered to be periodic. Therefore, under the condition that the P-wave velocity of the coal seam and the surrounding rock was constant, the period of the refracted P-wave was proportional to the coal thickness.

Modeling and simulation

In order to verify the periodicity of the refracted P-waves, three numerical models of panels with different coal thicknesses were established in this study. Each model consisted of three strata areas: roof, coal seam and floor. The parameters of the roof and floor were the same, and the specific parameters are shown in Table 1. The coal thicknesses of the three models were 20 m, 10 m and 5 m, respectively, and the plans and profiles are outlined in Fig. 3.

All models have the same size, 1000 m × 300 m × 30 m ($X \times Y \times Z$), with grid intervals of 1 m × 1 m × 0.5 m. All models contained two airways with a spacing of 200 m. The source was located in the middle of one airway, while the receivers were arranged in the other airway, with the spacing of 10 m. All of the sources and receivers were located close to the floor. The source signal was a 500 Hz Ricker wavelet, and the sampling time was 0.1 ms. A high-frequency source signal was selected to make wavelets narrow in time domain so as to clearly distinguish the periodicity of the refracted P-wave. The high-order staggered-grid finite difference method was applied for the three-dimensional simulations (He et al. 2017). The simulated Z-components of refracted P-waves are shown in Fig. 4.

It can be seen in Fig. 4 that the refracted P-waves have different periods in the simulated data of the different coal thickness models. Among those, the periods of the 20 m model and 10 m model could be read directly from the seismic records, at 18 ms and 9 ms, respectively, which was consistent with the results calculated by Eq. (3). However, for the 5 m model, since the period was less than the duration of the P-wave wavelet, the P-waves which had arrived at multiple times were observed to be overlapping, which caused the period to be unreadable in the seismic record. Therefore, although the refracted P-waves were periodic, this phenomenon had higher requirements on the thickness of coal seam and the frequency of source. However, for the

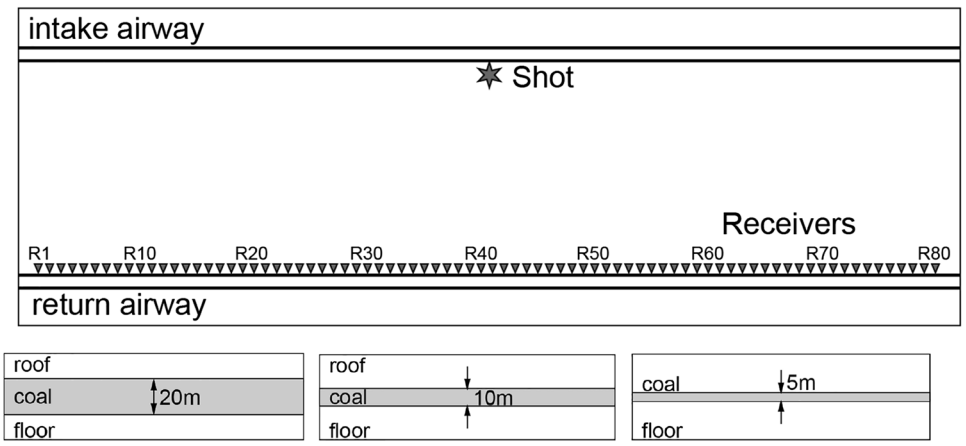

Fig. 3 Plans and profiles of the panel models

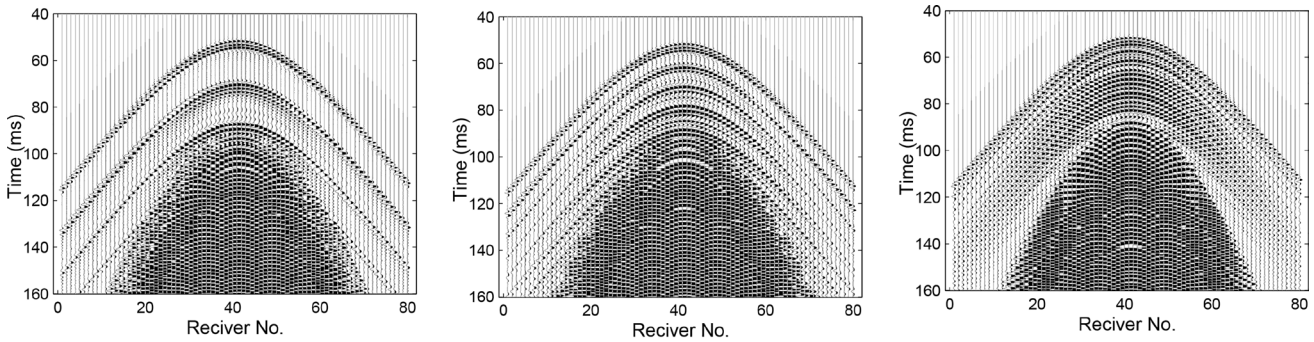

Fig. 4 Synthetic *Z*-components of refracted P-waves of models with different coal thicknesses

thick coal seams, the periods of the refracted P-waves could be obtained directly by using high-frequency sources, and the thicknesses of the coal seams could be accurately calculated. The determinations of the thicknesses of the coal seams were generally within 10 m. Therefore, it was found that in order to effectively measure the periods and obtain the thicknesses, it was necessary to process the data so as to eliminate the effects of aliasing.

It is important to place sources and receivers near either the roof or floor. For the same 20 m model, Fig. 5 shows the differences in the refracted P-waves under the conditions where all sources and receivers are located either at the bottom (Fig. 5a) or middle (Fig. 5b) of the coal seam. When located at the middle, receivers are affected by both upgoing and downgoing waves. Therefore, the period of refracted P-waves in Fig. 5 appears to be half of that in Fig. 5b. In addition, the upgoing and downgoing waves interfere with each other and take interference to refracted P-waves. This results in the noise being Fig. 5b is greater than that in Fig. 5a.

Algorithms and principles

It was found in this study that since the phases of the reflected waves and transmitted waves were constant under the condition of the critical angle, the wave form of the P-waves remained unchanged after multiple reflections and transmissions between the coal–rock interfaces. Therefore, the received refracted waves $s(t)$ could be regarded as the convolution of the source wavelet $w(t)$ with a sequence $a(t)$ as follows:

$$s(t) = w(t) * a(t), \tag{4}$$

where the sequence could be expressed as:

$$a(t) = \begin{cases} 1 & t = nT \\ 0 & t \neq nT. \end{cases} \tag{5}$$

The refracted waves $s(t)$ were recorded by the detector at the receiver point, and the source wavelets $w(t)$ were estimated from the signals recorded by the detector near the source. As $s(t)$ and $w(t)$ are known, many deconvolution methods can be applied to obtain $a(t)$, and then T can be calculated. However, if only one parameter T was estimated, a simpler method could be used.

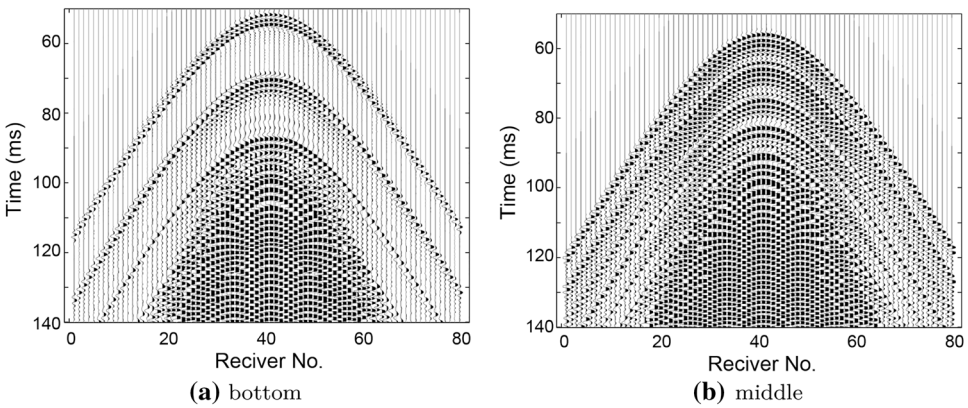

Fig. 5 Refracted P-waves of the 20 m model with different sources and receivers location

In order to estimate the source wavelets, this study first calculated the main frequency f_p of the signal acquired near the source point. Then, the source wavelet was approximated using a minimum phase wavelet $w(t)$ as follows:

$$w(t) = e^{-2\pi f_p^2 t^2 \ln(k)} \sin(2\pi f_p t), \tag{6}$$

where k is a factor of the amplitude attenuation, and its value can be selected between 1.5 and 2.5 according to the actual data.

Referring the geological conditions of the panel, an interval was set to limit the variations of the coal thicknesses. For each thicknesses value d in this interval, the period T was calculated using Eq. (3). Then, a sequence $a(t)$ was constructed with Eq. (4). Subsequently, $a(t)$ was convoluted with $w(t)$ to form a synthetic signal of the refracted wave $s(t)$. The error δ^2 between the synthetic signal $s(t)$ and the actual received signal $s_1(t)$ was then calculated using the following:

$$\delta^2 = \sum_{t=0}^{N} \left(s(t) - s_1(t)\right)^2, \tag{7}$$

where N indicates the wavelet length. After all of the values in the interval had been used to form the synthetic signals, the corresponding errors were calculated. The estimated coal thickness was d, which made the errors the minimum values.

As an example, the above method was applied to process the seismic data of the 5 m coal thickness model shown in Fig. 4. The source wavelet was constructed according to Eq. (6), where $k = 1.8$, and the main frequency was 500 Hz. The constructed source wavelet is shown in Fig. 6. The interval of the coal thickness was set between 1 and 20 m. All of the errors between the actual

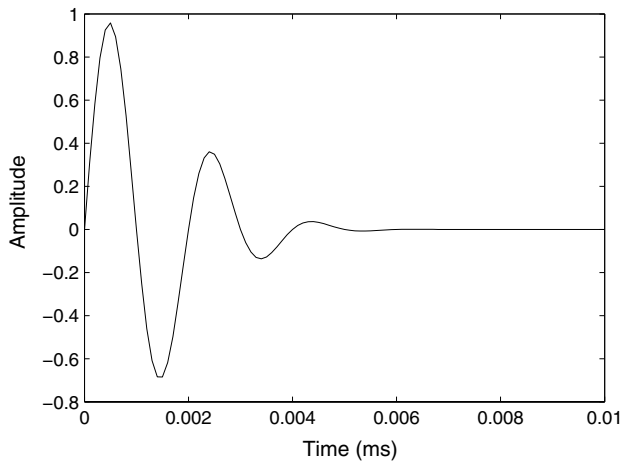

Fig. 6 Source wavelet with a main frequency of 500 Hz

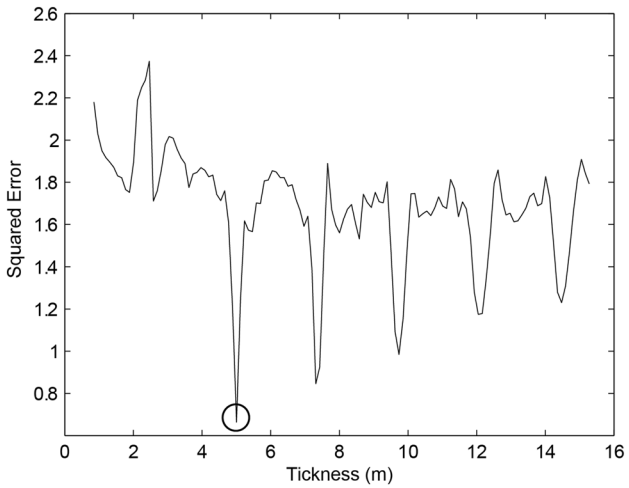

Fig. 7 Errors between the refracted P-wave signals of the 5 m model and the synthetic signals of the various coal thicknesses

refracted P-wave signals and the synthetic signals for the various thickness values are shown in Fig. 7. It can be seen that the minimum error occurred at 5 m, which was consistent with the coal thickness in that model. Figure 8 compares the synthetic signal of 5 m thickness with signal of the refracted P-wave from Fig. 4c.

Case study

The method proposed in the study was applied to a real case in order to assess its performance. The width of the No. 42224 panel in the Chaigou Mine was 122 m, and the average thickness of the coal seam was 7 m. In accordance with the airway exposure and borehole detection data, a scouting zone existed in the coal seam of the aforementioned panel. In order to verify the effectiveness of the proposed method for coal thickness detection, two positions are selected in the panel characterized with different coal thicknesses. There are two excitement shots (S1 and S2) in the intake airway. Several detectors (designated as R1 to R18) were arranged in the return airway for the purpose of receiving the seismic waves. All of the shots and detectors are located near the floor. The details of the observational system are shown in Fig. 9. Among the features, S1, R1,..., R9 were located in a normal area with approximately an 8 m coal thickness, while S2, R10,..., R18 were located in the scouting zone with approximately a 4 m coal thickness. R1 to R9 were received when S1 was excited, and R10 to R18 were received when S2 was excited. The coverage areas of the rays are shown in Fig. 9.

Shots S1 and S2 were excited within a 2 m hole with 120 g of explosive. The receivers R1 to R18 were embedded in holes with depths of 1 m and spacings of 20 m using

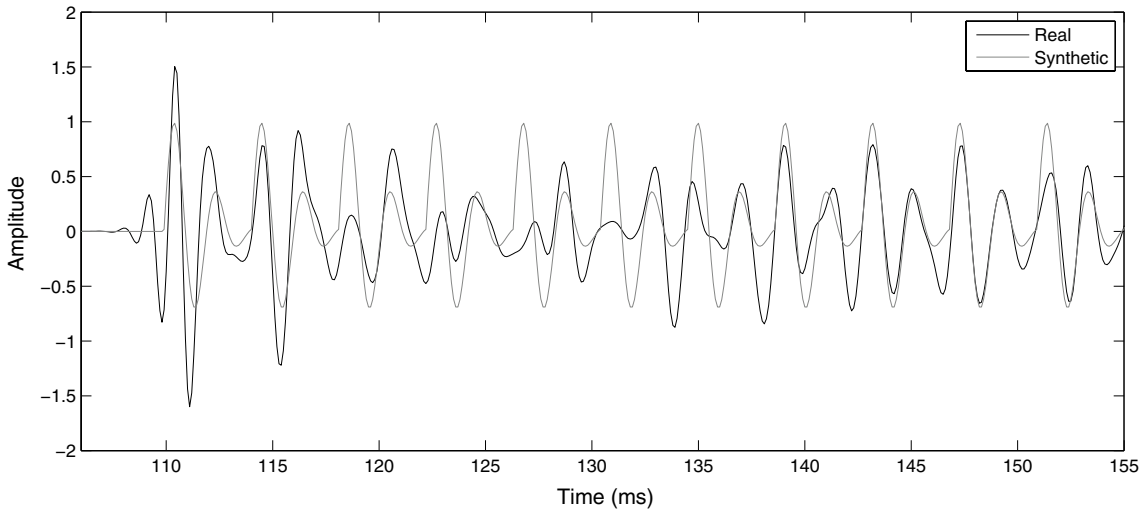

Fig. 8 Comparison of the synthetic signal of 5 m thickness with the signal of refracted P-wave from the 5 m model

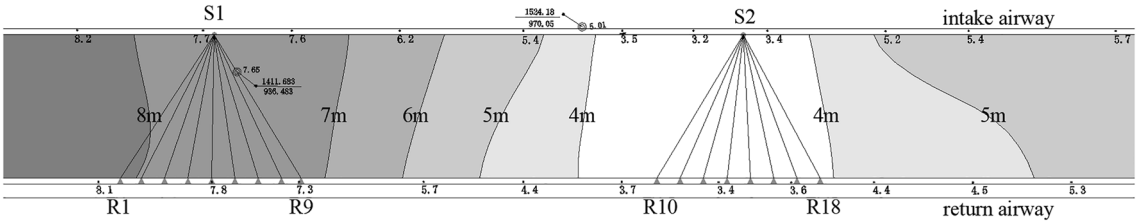

Fig. 9 Distribution of the coal thicknesses in the No. 42224 panel and the layout of the observational system

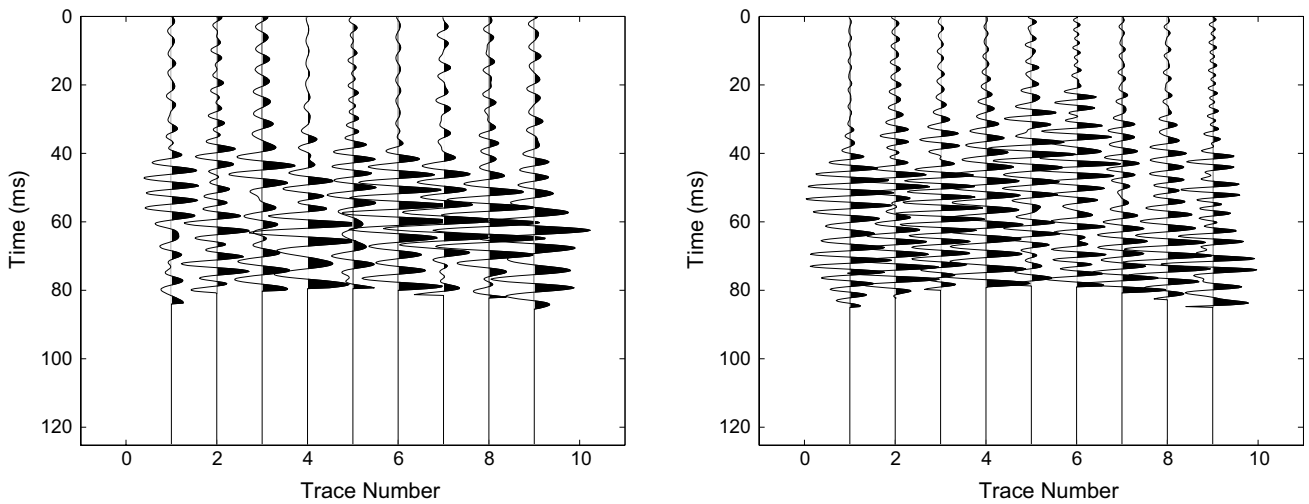

Fig. 10 The refracted P-waves of S1 (left) and S2 (right)

Z-component detectors. After pre-processing the received seismic data, this study uses 4200 m/s as the P-wave velocity of the surrounding rock for the purpose of calculating the first arrival times t_0 and to cut off the data after $t_0 + 40$ ms in order to retain the refracted P-wave only. The refracted P-waves of S1 and S2 are shown in Fig. 10. It can be seen that frequency of the S1 signals was general slightly lower than that of the S2 signals.

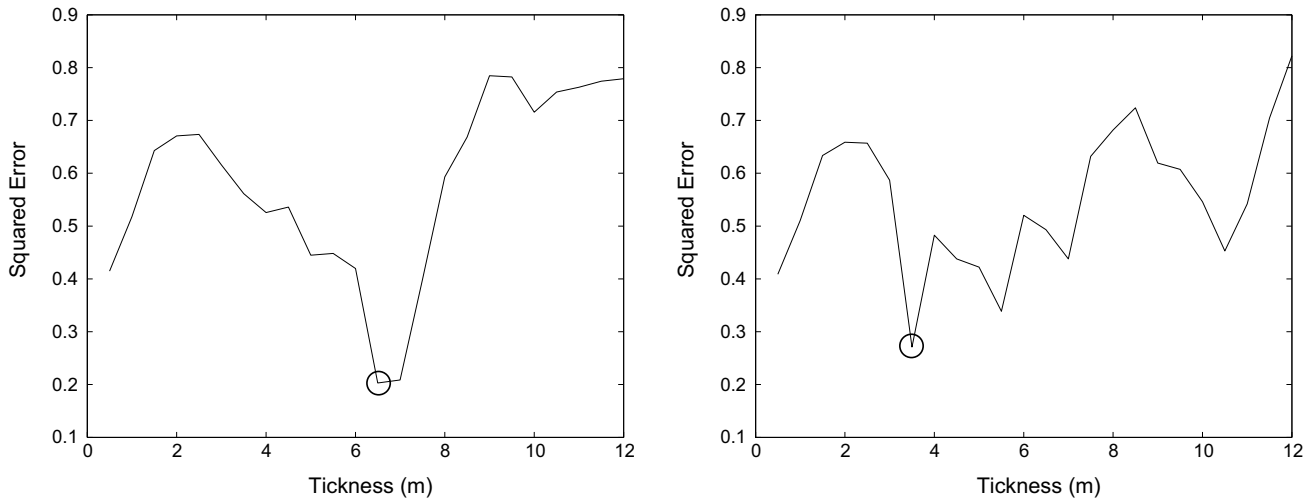

Fig. 11 Errors between the synthetic signals of the various coal thicknesses and the refracted P-waves of S1 (left) and S2 (right)

The data acquired from the detectors placed near Points S1 and S2 were analyzed, and 260 Hz was selected as the main frequency for generating the source wavelets and process the signals of S1 and S2 using the proposed method. The errors between the actual refracted P-wave signals and the synthetic signals of the various coal thicknesses obtained according to Eq. (4) are shown in Fig. 11. It can be seen from the figure that the minimum error was reached when the coal thickness was 3.8 m for S1 and 7 m for S2, which was found to be consistent with the actual geology. Figure 12 details comparison of the actual signal of the trace R7 with the synthetic signal at 3.8 m, as well as comparison of the signal of the trace R12 with that at 7 m. It can be seen that the synthesized signals of the appropriate coal thicknesses had been in good agreement with the actual P-wave signals.

Conclusions

The seismic waves which are excited and received in coal seams include both refracted P- and S-waves. The apparent velocity of the refracted P-wave has been found to be close to the P-wave velocity of the surrounding rocks, yet displays strong periodicity characteristics. These periods have been determined to be proportional to the thicknesses of the coal seams. The reason for this phenomenon is that the amplitudes of the transmitted P-waves and reflected P-waves reach the maximum values at the same time only when the incident angle is the critical angle. Therefore, P-waves can be reflected multiple times at the critical angle between two coal–rock interfaces. In addition, each reflection produces a strong transmission wave passing along the interface. Therefore, the received refracted P-waves have strong periodicity. This study's simulations of various coal thicknesses using various models showed that the periodicity of the refracted P-waves could be directly observed when excited by focused high frequency in thick coal seams. The coal thicknesses could be simply calculated by the period. However, it was found that in thin- or medium-thick coal seams, the multiple transmitted P-waves tended to overlap, making it difficult to directly perform estimations. In order to address these issues, this study first composed the source wavelets and then composite synthetic P-waves of various coal thicknesses. It was found that the suitable estimated coal thicknesses corresponded to the minimum values of the errors between the synthetic and actual refracted P-waves.

In this study, three assumptions were made in order to simplify the processes of wave formation and propagation:

1. The lithology of roof and floor strata was considered to be the same. If the differences were significant, then the two critical angles on the coal–rock interfaces would also differ greatly.
2. The two interfaces were parallel to each other. This condition ensured that the reflected waves on one interface would occur at the critical angle on the other interface.
3. The coal thicknesses between the source point and the receiving point were constant. As a result, the coal thicknesses estimated by the proposed method could be regarded as the average thicknesses of the coal seam between those two points.

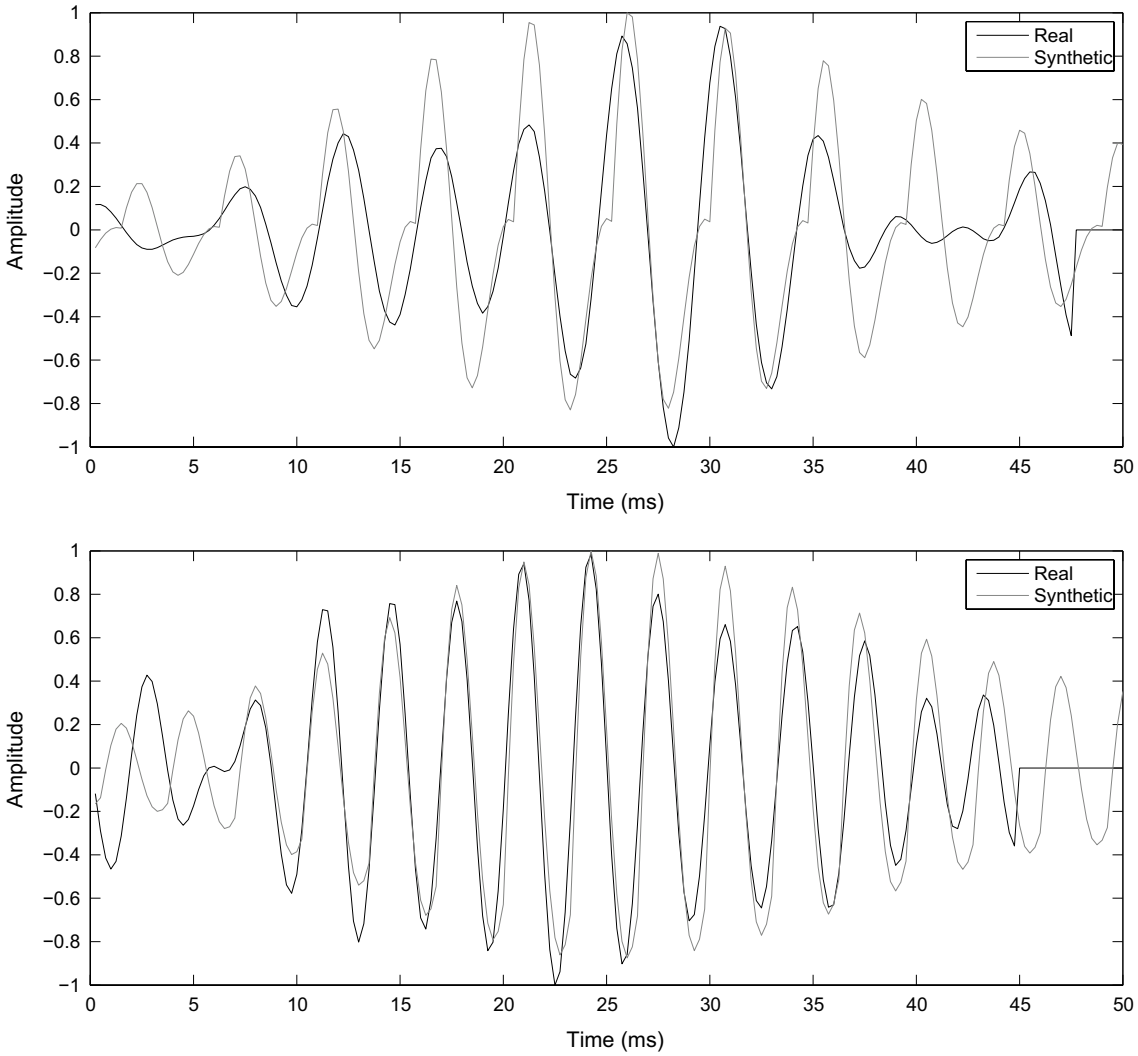

Fig. 12 Comparison of the synthetic signal with the actual signal from S1 (up) and S2 (down)

The local variations of the coal seams in regard to lithology, dip angles and thicknesses will result in local changes in the amplitudes and periodicity of the refracted P-waves. Therefore, it should be considered feasible to use the refracted P-waves to predict the thickness distributions of coal seams in mining panels in the future.

Acknowledgements This research has been performed under the National Key Research and Development Plan of China (No. 2018YFC0807804) and National Natural Science Foundation of China (No. 41974209).

Compliance with ethical standards

Conflict of interest The authors declare that they have no conflict of interest.

References

Buchanan DJ (1978) The propagation of attenuated SH channel waves. Geophys Prospect 26(1):16–28

Gritto R (2003) Subsurface void detection using seismic tomographic imaging. Lawrence Berkeley National Laboratory, Berkeley

He W, Ji G, Dong S et al (2017) Theoretical basis and application of vertical Z-component in-seam wave exploration. J Appl Geophys 138:91–101

Hu Z, Zhang P, Xu G (2018) Dispersion features of transmitted channel waves and inversion of coal seam thickness. Acta Geophys 66(5):1001–1009

Ji G, Cheng J, Hu J (2014) In-seam wave imaging using attenuation coefficient: method and application. J China Coal Soc 39(S2):471–475 (**in Chinese**)

Krey TC (1963) Channel waves as a tool of applied geophysics in coal mining. Geophysics 28(5):701–714

Liu S, Zhang J, Li C (2019) Method and test of mine seismic multi-wave and multi-component. J China Coal Soc 44(01):271–277 (**in Chinese**)

Liu S, Zhao W, Gao S (2019) Experimental study on coal seam thickness measurement of ultra-wide band ground penetrating radar. Coal Sci Technol 47(08):207–212 (**in Chinese**)

RÄDer D, Schott W, Dresen L et al (1985) Calculation of dispersion curves and amplitude-depth distributions of Love channel waves in horizontally layered media. Geophys Prospect 33:800–816

Regueiro SJ (1990) Seam waves: what are they used for? Part 2. Lead Edge 9(8):32–34

Schott W, Waclawik P (2015) On the quantitative determination of coal seam thickness by means of in-seam seismic surveys. Can Geotech J 52(10):1496–1504

Sheriff RE, Geldart LP (1995) Exploration seismology, 2nd edn. Cambridge Univ. Press, Cambridge

Wang B, Liu S, Jiang Z et al (2011) Advanced forecast of coal seam thickness variation by integrated geophysical method in the laneway. Procedia Eng 26:335–342

Wang G, Pang Y, Ren H (2020a) Intelligent coal mining pattern and technological path. J Min Strata Control Eng 2(01):5–19 (**in Chinese**)

Wang J, Liu Z, Niu H (2020b) Study on influence of collapse columns on refracted waves between coal seam and rocks and corresponding tomography method. Coal Sci Technol 48(02):214–219 (**in Chinese**)

Yancey DJ, Imhof MG, Feddock JE et al (2007) Analysis and application of coal-seam seismic waves for detecting abandoned mines. Geophysics 72(5):M7–M15

Zhang J, Liu S, Wang B et al (2019) Response of triaxial velocity and acceleration geophones to channel waves in a 1-m thick coal seam. J Appl Geophys 166(166):112–121

Zhu M, Cheng J, Cui W et al (2019) Comprehensive prediction of coal seam thickness by using in-seam seismic surveys and Bayesian kriging. Acta Geophys 67(3):825–836